Comparison Between Sea Surface Wind Speed Estimates From Reflected GPS Signals and Buoy Measurements

James L. Garrison
NASA Goddard Space Flight,Greenbelt, MD, 20707
(301)286-8204, (301)286-0369(fax), james.l.garrison.1@gsfc.nasa.gov
Stephen J. Katzberg
NASA Langley Research Center, Hampton, VA, 23681
Valery U. Zavorotny
CIRES/NOAA Environmental Technology Laboratory, Boulder, CO, 80303-3328
Dallas Masters
University of Colorado at Boulder

ABSTRACT

Reflected signals from the Global Positioning System (GPS) have been collected from an aircraft at approximately 3.7 km altitude on 5 different days. Estimation of surface wind speed by matching the shape of the reflected signal correlation function against analytical models was demonstrated. Wind speed obtained from this method agreed with that recorded from buoys to with a bias of less than 0.1 m/s, and with a standard deviation of 1.3 meters per second.

INTRODUCTION

The use of bistatically scattered signals from the Global Positioning System (GPS) as a radar remote sensing instrument for sea surface roughness is presently being studied by researchers at several different institutions. Reflected GPS data was recently collected from an aircraft during March of 1999 in conjunction with the Space and Naval Warfare Systems Command (SPAWAR) Electro-Optical Propagation Assessment in Coastal Environments (EOPACE) program. These flights provided direct comparison between measurements using reflected GPS signals and those data obtained from recording buoys.

MEASUREMENT TECHNIQUE

Pseudorandom noise (PRN) codes used in satellite navigation systems are designed to have an autocorrelation function which has large values only for lags within 1 chip of zero. (A "chip" is the time between bit transitions.) Reflection of this incident signal from a surface which has a random distribution in slopes will result in a signal composed of a distribution in path length delays. The cross correlation between a localy generated PRN code and this reflected signal will result in a function which is wider than the autocorrelation of the direct signal. Qualitatively, a higher mean square slope of surface facets will result in a wider cross-correlation function. The physical relationship between the sea surface wind speed and surface slope statistics has been well established [1]. Therefore recording the shape of the cross correlation function from reflected PRN coded signals can be used as a measurement of surface wind speed. Analytical and empirical models have been generated for this dependence [2], [3] and applied to the problem of retrieval of wind speeds from bistatically scattered GPS signals [4].

INSTRUMENTATION

A modified GPS receiver was used to track the direct line of sight satellites through a zenith-oriented right hand circularly polarized (RHCP) antenna and record the cross-correlation function of the reflected signals using a nadir-oriented left hand circularly polarized (LHCP) antenna. The cross-correlation for one or two satellites was continuously recorded in 10 to 12 range bins. Accumulation was done in hardware for an integration time of 1 ms. Batches of 0.1 seconds of the sum square of the inphase and quadrature components were then averaged before being saved to disk.

An Ashtech Z-12 receiver was also carried on the aircraft in order to obtain geolocation data for later postprocessing. Precise GPS ephemerides from the National Geodetic Survey were also obtained for the days of the flights.

DATA COLLECTION CAMPAIGNS

The NASA Langley Research Center B-200 aircraft was used to carry this instrument on five different days (March 1, 5, 8, 11 and 12, 1999) during the EOPACE experiment. A similar flight path was followed on each day. Surface truth data was available from this experiment at three different locations: the Duck meteorological station (DUCN7), and two research buoys provided for this experiment (identified as the "Flux" and "Met" buoy).

PROCESSING

Post processing was performed to accomplish two functions: determining the location of the specular reflection point and realigning each correlator sample relative to the specular point. This was done to reference the specular point to the location of ground truth and to continuously map the waveform samples at finer than 1/2 chip precision.

This realignment was performed through use of the navigation data from the Ashtech receiver and the NGS ephermides.

The true path length difference between a direct and reflected signal from a given satellite was found by minimizing the total path length of a reflected signal, subject to the constraint that the specular point lie on the WGS-84 ellipsoid.

A constant noise floor, determined using the theoretical value set by the AGC prior to digital sampling was subtracted from all correlation measurements before the constant area normalization was performed. The waveform power was then normalized to have a constant total area of one half code chip by dividing by the total integrated power in all range bins at each waveform sample. This removes changes in the intensity of the incident radiation and was also found to produce results with a lower variance. It also eliminates many uncalibrated effects such as aircraft attitude motion and the antenna gain pattern.

The result of post-processing was a standard set of "level 1a" data. This consists of sets of normalized correlation power $Y_k^2(\delta_i)$ at specific code delays, $\delta_{k,i}$. For each k^{TH} waveform sample, taken at a 10 Hz rate, auxiliary information giving the specular point location (ϕ_{S_k}, λ_{S_k}) and the GMT of the measurement are also included in the level 1a data set.

RETRIEVAL TECHNIQUE

The analytical model from Zavorotny and Voronovich [2] was used to generate theoretical shapes of the normalized waveform at different wind speeds, aircraft altitudes and GPS satellite elevations. The effects of Doppler were ignored for these experiments because of the low aircraft speed. Fully-developed seas ($\Omega = 0.84$) were assumed.

Performing the complete integration required by this model at each point during every interation step called by the estimator would have been computationally intensive. For that reason, this integration was approximated by an 8th order series in terms of wind speed (V_w) and code delay (δ) having the following form.

$$Y^2(\delta) \approx S \exp\left[\sum_{i=0}^{N}\sum_{j=0}^{M} a_{i,j} V_w^j (\delta - \delta_0)^i\right] \qquad (1)$$

Three parameters: wind speed V_w delay of the peak of the waveform from the computed specular point, δ_0 and the scale factor S were estimated using a nonlinear least squares method to batch segments of waveform data (δ_k, Y_k^2). The least squares minimization problem was solved through a large-scale optimization subroutine provided in the optimization toolbox in MATLAB [5].

Although each waveform sample was scaled to have a constant area of one half chip, the scale factor (S) was found to improve the estimation accuracy. This was postulated to be the result of the finite number of delay not recording the complete waveform because portions of the trailing edge often extend beyond the range of these bins. The scale factor therefore accounts for the fact that the measured waveform, once scaled to be constant area, has slightly larger area than that predicted by theory. The parameter δ_0 accounted for the uncalibrated path length delays between direct and reflected signal paths, and the sea surface height relative to the ellipsoid.

Three effects and receiver anomalies were identified in the data and either corrected or edited from batch before processing by the least squares estimator. Editing the data in this manner was found to improve the performance of this estimator and removed most of the wind speed estimate outliers.

First, if the total power in all delay bins fell below a threshold, then the complete waveform was rejected. This eliminated measurements made over land, and time in which the receiver had not acquired a strong reflected signal. Second, occasional slips by an integer number of half code chips in the spacing of the delay bins was observed. This anomaly was detected by searching for discontinuities in the waveform centroid

$$\tau_{c_k} = \frac{\sum_i Y^2(\tau_{k,i})\tau_{k,i}}{\sum_i Y^2(\tau_{k,i})} \qquad (2)$$

The third effect which was identified were instances in which the leading edge of the waveform extends earlier than the first correlator, resulting in signal power in the first (noise floor) bin. Attempts to fit the function (1) to these data resulted in a wider than required waveform shape and consequently a higher wind speed. Individual waveforms in which this correlation power exceeds a threshold were deleted from the ensemble. Although most of the information about the surface slope statistics is contained in the trailing edge of the waveform, the functional form of (1) was sensitive to the waveform shape returning to zero earlier than 1 chip before the specular point.

Finally, a residual monitoring process is used in which a threshold is set on the sum square of residuals in one waveform. This was computed from the difference between the observed and computed power following the least squares estimate for the k^{TH} waveform.

$$r_k = \sum_i (Y_{k,i}^2 - Y_c^2(\delta_{k,i}, V_w, S, \delta_0))^2 \qquad (3)$$

in which Y_c^2 is the function from equation (1) computed with the estimates of V_w, S, and δ_0. The k^{TH} waveform was rejected from the ensemble when r_k exceeded a threshold (set by experimentation). The complete batch of data (less the waveforms which were rejected) was then processed through the least squares estimator a second time. Residuals were computed for the second pass, and were used to manually identify examples of poor fits. For the data presented in this paper, there was only one example of an estimate rejected as the result of high residuals following the second pass through the estimator.

DATA ANALYSIS

Segments of data in which the specular point of the reflection was near to a buoy were used to evaluate the accuracy of wind speed retrieval. The Flux Buoy was 10 km from the shore

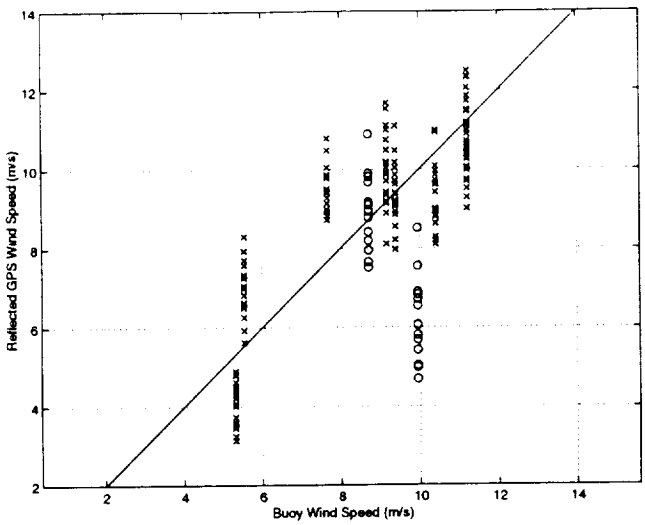

Figure 1: Comparison of Wind Speed obtained from Reflected GPS Measurements with that from Recording Buoys.

and was expected to give the best comparison with nearby measurements. However, this buoy was not functioning during the flights of March 11 and 12, so the Met buoy (closer to the shore) was used for comparison on those days. Wind direction was obtained from the Duck meteorological station. Sets of 100 seconds of data, approximately centered at the Flux Buoy location, were used in these comparisons. Batches of 5 seconds of waveform data from these segments were processed to obtain each state estimate. A set of coefficients $a_{i,j}$ were computed for the series in (1) at the aircraft altitude and the average elevation during the time that the buoy overflights were taken. Only satellites with an elevation greater than 30 degrees were considered. Results from the buoy comparison are shown in Figure 1. The bias and standard deviation of this complete set of comparison measurements was 0.09 m/s and 1.3 m/s, respectively.

Table 1 lists relevant data for the 5 days of this experiment used to generate the comparison in Figure 1. Note that on March 1, 1999 (the data indicated by an "O" on Figure 1) the wind was from the East (272 degrees). The large error in that set of measurements may be therefore be explained by not fully developed seas.

CONCLUSIONS

These results have demonstrated that, from aircraft altitudes, reflected GPS signals can provide remotely sensed wind speed measurements of comparable precision to other existing, active instruments (such as scatterometers). Furthermore, the retrievals presented in this paper were performed by inverting an analytical model. There was no calibration, or adjustment of this model required. For a satellite based instrument, however, additional effects must be considered, such as Doppler,

Table 1: Summary of Buoy Comparisons

Date	Wind Dir. (deg.)	Wind Spd. (m/s)	GPS Sat. PRN	Alt. (km)	Elev. (deg.)
3-1-99	272	8.7	15	3.7	54
		9.9	27		40
3-5-99	20	5.3	18	3.7	33
		5.3	19		70
3-8-99	355	11.2	19	3.6	67
		9.4	19		73
		11.2	31	3.6	83
		9.2	31		75
3-11-99	323	7.7	31	3.7	83
3-12-99	327	10.4	31	3.7	82

the larger glistening surface, and the lower signal to noise ratio. Nonetheless, the comparison demonstrated during this experiment would serve to validate the analytical models used in predicting instrument performance in a satellite orbit.

REFERENCES

[1] Cox, C. and Munk, W., Measurement of the Roughness of the Sea Surface from Photographs of the Sun's Glitter, *Journal of the Optical Society of America*, Vol. 44, No. 11, pp. 838-850, November 1954.

[2] Zavorotny, V. U., and Voronovich, A.G., Scattering of GPS signals from the ocean with wind remote sensing application, *IEEE Trans. Geosci. Remote Sens.*, Vol. 38, No. 2, pp 951-964, March 2000.

[3] Lin, B., Katzberg, S. J., Garrison, J. L., and Wielicki, B., The Relationship Between the GPS Signals Reflected from Sea Surfaces and the Surface Winds: Modeling Results and Comparisons With Aircraft Measurements, *Journal of Geophysical Research - Oceans*, in press.

[4] Clifford, S.F., V.I.Tatarskii, A. G. Voronovich and V.U.Zavorotny, "GPS Sounding of Ocean Surface Waves: Theoretical Assesment,in *Proceedings of the IEEE International Geoscience and Remote Sensing Symposium: Sensing and Managing the Environment*, pp. 2005-2007, IEEE, Piscataway, N. J., 1998.

[5] MATLAB Optimization Toolbox Users Guide, The MathWorks, Inc., Natik, MA, pp 2-20,2-21, 1997.